

## MODELING OF AGGLOMERATION IN A FLUIDIZED BED

A. Rehmat, C. Huang,\* R. Carty

Institute of Gas Technology  
Chicago, Illinois 60616

H. Hariri, H. Arastoopour

Illinois Institute of Technology  
Chicago, Illinois 60616

### ABSTRACT

A fluidized bed containing a central jet was operated with low-temperature melting materials to obtain the rate of agglomeration as well as to measure the temperature distribution within the fluidized bed. The rate of agglomeration was obtained as a function of operating parameters such as temperature and velocity. The agglomeration rate defined, as the rate of change in the number of particles of a particular size, was determined from the particle population balance using the experimental data.

The agglomeration model developed to predict the agglomeration rate constant based on the temperature distribution in the fluidized bed and the rate of entrainment of particles into the jet yielded values for the rate constants similar to the experimental values.

### INTRODUCTION

Fluidized-bed systems have been used in many coal conversion and other chemical processes. The fluidized beds are sometimes operated under agglomerating conditions to maximize coal utilization. The operating conditions in such cases are chosen to prevent the onset of sinters and defluidization (1,2,3,4). Under suitable operating conditions, ash agglomeration provides a very effective means of ash removal from a coal gasifier (5).

A distinguishing feature of an ash-agglomerating coal gasifier is a region where the temperature of the ash particles is high enough to make the surfaces sticky so that when they collide with each other, they adhere to each other to produce agglomerates. The rate of the formation of these agglomerates depends upon several factors such as the oxidant distribution within the bed, the overall fluidization velocity, and the ash properties. The oxidant distribution primarily influence the formation of the localized zone of high temperature within the fluidized bed, whereas the velocity influences the rate of particle collision as well as the particle entrainment within this zone. Based on these factors, a mathematical model for agglomeration has been developed to predict the rate of agglomeration in a fluidized bed containing a central jet. These rates are then compared with those obtained from the actual experiments.

### EXPERIMENTAL APPARATUS AND PROCEDURE

The apparatus consists of a 15.2-cm-ID glass fluidized-bed column, a metal section positioned beneath the glass column for temperature measurement and sampling, a gas distributor, a jet and fluidizing air heating system, temperature controlling and temperature measurement devices, and flow regulation and measurement systems (Figure 1). In the experiment, the jet and the fluidizing air temperatures

---

\*Dr. Huang is currently at Nalco Chemical, Naperville, Illinois.

were varied and the temperature distribution and the agglomeration of the particles in the bed were measured. Polyethylene and polyolefin particles were used as bed material. Two types of gas distributors were used: a flat porous plate with a central jet and a porous cone with a central jet.

The jet gas temperature was adjusted to a value above the melting temperature of the bed material. The fluidizing air (auxiliary air) temperature was generally maintained lower than the softening temperature of the bed material to avoid sinter formation on the distributor.

#### EXPERIMENTAL RESULTS

Figure 2 shows the effect of jet temperature on the agglomeration for a flat porous distributor with high-density polyethylene bed material. The measure of agglomeration is the weight percentage of particles greater than 850  $\mu\text{m}$ , which increased linearly with residence time at each temperature level. The percentage of agglomerates also increased linearly with the fluidizing gas and bed temperatures; however, the jet air temperature was found to have the most significant effect on the agglomeration rate.

Another important factor affecting the rate of agglomeration in fluidized beds is the rate of particle entrainment into the high-temperature jet region. The entrainment rate depends on the stress distribution among the particles in the vicinity of the jet region. The direction, magnitude, and component of the stress toward the jet region depends on the cone angle. Figure 3 compares the agglomeration obtained with gas distributors having half-cone angles of 30°, 45°, 60°, and 90° (flat) after 2, 4, 6, and 8 hours of steady-state operation. The agglomeration increased as the cone angle decreased up to 45°. However, when the cone angle was decreased to 30°, the agglomeration was found to be less than that with cone angle of 45°. This implies that, although the steeper inverted cone directed the stress on the particles in the cone section more effectively toward the jet zone, the amount of particles in the cone section decreased resulting in lower entrainment of the particles. Because of this competitive effect, there exists an optimum cone angle for the maximum rate of agglomeration. This half-cone angle is approximately 45°. The optimum angle can be a function of particle-size distribution, shape and surface roughness of the particles, and the jet and the fluidizing air velocities.

The temperature distribution inside the bed was plotted using temperature measurements at more than 50 locations inside the fluidized bed. A typical temperature distribution profile in the area near the porous cone distributor is illustrated in Figure 4. More data concerning other operating conditions are given elsewhere. (6).

#### DATA ANALYSIS

In a fluidized bed operated under agglomerating conditions, the rate of agglomeration between particles of two different sizes is proportional to the product of their concentrations. The proportionality constant is called the agglomeration rate constant.

To define the rate of agglomeration, we have adopted a definition that is analogous to the rate of chemical reaction. In a chemical reaction, the rate of reaction is defined in terms of the rate of change in the number of moles of a particular component in the reacting system due to its reaction. In the agglomeration process, what is changed during the process is the particle-size distribution. Therefore, it is appropriate to define the rate of agglomeration of particles of a particular size as the rate of change in the number of particles of that size. Due to the difficulty in measuring the number of particles of a particular size per unit volume of the fluidized bed, it has been found convenient

to express the rate of agglomeration of the particles in terms of its rate of change per unit mass of the bed material.

Since the overall rate of agglomeration is a measure of the rate of change in the number of particles of various sizes, the particle size is defined in a manner that is meaningful and facilitates the numerical computation in the particle population balance. It is assumed that all particles are made up of unit particles of mass  $m_0$  and diameter  $d_0$ . This assumption implies that particle size is discrete and each particle has a mass equal to an integer times the mass of a unit particle. The particle whose mass is  $I$  times the mass of a unit particle ( $I \times m_0$ ) is called particle size  $I$ .  $N(I)$  is defined as the number of particles of size  $I$  per unit mass of bed material and is called the mass number density of particles of size  $I$ . The rate of agglomeration of particles of size  $I$  can be expressed as:

$$R(I) = \frac{dN(I)}{dt} \quad 1)$$

The value of the rate of agglomeration  $R(I)$  is dependent upon operating variables, including the temperature distribution in the bed, velocity, and particle-size distribution.

If we assume the agglomeration process as involving the collision of a single particle of size  $I$  and a single particle of size  $J$ , then it is reasonable to assume that the generation rate of agglomerates ( $I + J$ ) forming from particles of size  $I$  and particles of size  $J$  is proportional to the collision frequency between these particles. As the number of collisions between particles of any two particular sizes is proportional to the product of their mass number densities, the rate of generation of agglomerates of size  $(I + J)$  from particles of sizes  $I$  and  $J$  is:

$$R_{I,J} = K_{I,J} N(I) N(J) \quad 2)$$

Here,  $K_{I,J}$  is the agglomeration rate constant.

Particle Population Balance for Batch Process. In the population balance of the particles of a particular size  $I$ , all the possible combinations leading to the formation or consumption of size  $I$  particles are to be considered since particles of size  $I$  combines with other particles to form agglomerates of larger sizes; on the other hand, smaller particles may stick together and form agglomerates of size  $I$ . Using Equation 1, the rate of generation of agglomerates of size  $I$  from smaller particles is:

$$\frac{1}{2} \sum_{J=1}^I K_{I-J,J} N(J) N(I-J)$$

Similarly, the rate of consumption of particles of size  $I$  due to agglomeration is:

$$\sum_{J=1}^L K_{I,J} N(I) N(J)$$

where  $L$  is the size of the largest particles that exist in the bed. The population balance for particles of size  $I$  in batch process can thus be written as:

$$\frac{\partial N(I)}{\partial t} = \frac{1}{2} \sum_{J=1}^I K_{I-J,J} N(J) N(I-J) - \sum_{J=1}^L K_{I,J} N(I) N(J) \quad 3)$$

Computation of Agglomeration Rate Constant. For the computation of the agglomeration rate constant from the data, it is first expressed in terms of the operating variables and particle sizes. This approach facilitates in solving the rate constant integral equations. The agglomeration rate constant  $K_{I,J}$  can be

represented by the product of two functions; the first function,  $k_{op}$ , is dependent upon the operating conditions, and the other,  $k(d_I, d_J)$ , is size-dependent, as:

$$K_{I,J} = k_{op} k(d_I, d_J) \quad (4)$$

It is difficult to obtain an expression for  $k(d_I, d_J)$  from a theoretical standpoint. Based on the behavior of particles, one restriction that can be imposed on the functional form of  $k(d_I, d_J)$  is that it should be symmetric with respect to  $d_I$  and  $d_J$ . The ultimate functional form of  $k(d_I, d_J)$  must be determined with the aid of experimental data.

Even with the assumptions of Equation 4, there are still too many possible combinations of  $k_{op}$  and  $k(d_I, d_J)$  to be tested, and further simplification of the testing procedure is needed. To achieve this, the particle population balance Equation 3, for a specific operating condition, is rearranged as follows:

$$k_{op} = [MN(I)/Mt] / \left[ \frac{1}{2} \sum_{I=1}^I k(d_{I-J}, d_J) N(J) N(I-J) d_J - \sum_{I=1}^L k(d_I, d_J) N(I) N(J) d_J \right] \quad (5)$$

Thus, if the correct functional form of  $k(d_I, d_J)$  is used in Equation 5, the calculated  $k_{op}$  should have the same value for all of the particle sizes under specific operating conditions. This provides a means to test the functional form of  $k(d_I, d_J)$ . To find the correct functional form of  $k(d_I, d_J)$ , several symmetric functions with respect to  $d_I$  and  $d_J$  were substituted into Equation 5. Our studies showed that the functional form of

$$(d_I^4 + d_J^4) \left( \frac{1}{d_I^3} + \frac{1}{d_J^3} \right)$$

results in a nearly constant value of  $k_{op}$  over the whole particle size range at specific operating conditions. Therefore,  $K_{I,J}$  can be expressed as:

$$K_{I,J} = k_{op} (d_I^4 + d_J^4) \left( \frac{1}{d_I^3} + \frac{1}{d_J^3} \right) \quad (6)$$

The experimental data was used to calculate  $MN(I)/Mt$ ; then the agglomeration rate constant  $k_{op}$  was calculated using Equations 5 and 6. These values at different jet temperatures are shown in Table 1.

Table 1. THE CALCULATED VALUES OF  $k_{op}$  BY PARTICLE POPULATION BALANCE USING EXPERIMENTAL DATA

Jet Temp, °C	144.4	143.3	142.8	142.2
$k_{op}$	$1.78 \times 10^{-9}$	$1.20 \times 10^{-9}$	$0.9 \times 10^{-9}$	$0.45 \times 10^{-9}$

The value of  $k_{op}$  increases significantly with a slight increase in jet temperature (Table 1 and Figure 2).

#### AGGLOMERATION MODEL

As the hot jet gas stream is fed into the fluidized bed through the nozzle at a temperature substantially higher than the fluidizing gas temperature, a hot jet zone in the central portion of the bed is created. The concentration of solids in the jet zone is much lower than the solids concentration in the bulk of the bed. The solid particles enter the jet zone and exchange heat with the hot jet gas. The temperature of the particles in the jet zone increases; for some particles, this

results in partial melting. Upon the collision of two sticky particles, agglomeration may occur. Whether agglomeration takes place or not depends on several particle characteristics, including the relative velocity of the colliding particles, the thickness of the molten layer, and the viscosity of the molten material.

In the area near the jet, the particles are assumed to travel horizontally as they are entrained into the jet until they reach the jet boundary where particles enter into the jet zone and travel upward and finally exit from the top of the jet.

The entrainment of gas into a free jet has been given by Ricou and Spalding (7) as:

$$\frac{M_g}{M_{go}} = 0.32 \left( \frac{x}{d_n} \right) \left( \frac{\rho_{g1}}{\rho_{go}} \right)^{1/2} \quad (7)$$

where —

$M_{go}$  = mass flow rate of initial jet gas, kg/h

$M_g$  = mass flow rate of initial and entrained gas, kg/h

$x$  = distance from nozzle exit, m

$d_n$  = nozzle diameter, m

$\rho_{g1}$  = density of entrained gas, kg/m<sup>3</sup>

$\rho_{go}$  = density of gas exiting nozzle, kg/m<sup>3</sup>

The presence of particles may affect the entrainment of gas into the jet stream. However, this effect was found to be negligible for the particle-size range (mean particle diameter = 350  $\mu$ m) used in this study (8). The particles are entrained near the jet by the entrained gas; then they change direction and move upward due to momentum exchange with the jet gas. In this study, the flow of gas entrained to the jet is negligible in comparison with the jet gas flow rate. However, the rate of gas entrainment has been used to estimate the particle entrainment into the jet. As the particles enter into the jet, they travel upward due to the jet gas momentum. The following momentum balance was used to calculate the particle velocity in the jet zone.

$$\epsilon_p \rho_p v_p \frac{dv_p}{dx} = \frac{3}{4} C_D \frac{\rho_g (v_g - v_p)^2}{g_c d_p} (1 - \epsilon_p)^{-2.6} - (\rho_p - \rho_g)g \quad (8)$$

where  $x = 0$  defines the location where the particles enter the jet zone.  $v_p$  and  $v_g$  are particle and gas velocities, respectively,  $\epsilon_p$  is the particles void fraction, and  $C_D$  is the drag coefficient.

With the assumption that heat transfer to a particle is via heat exchange with its surrounding gas stream, the heat balance on a single particle in the region near and in the jet is expressed as:

$$\frac{\partial T_p}{\partial t} = \alpha \left[ -\frac{1}{r} \frac{\partial}{\partial r} \left( r^2 \frac{\partial T_p}{\partial r} \right) \right] \quad (9)$$

where  $\alpha$  is the particle thermal diffusivity.

$$\text{at } t = 0, T_p = T_B \quad (10)$$

where  $T_B$  is the bed temperature

$$\text{at } r = 0, \frac{\partial T}{\partial r} = 0 \quad (11)$$

and

$$\text{at } r = R, K_S \frac{\partial T}{\partial r} = \begin{cases} h(T_v - T_p) & \text{near the jet} \\ h(T_j - T_p) & \text{at the jet zone} \end{cases} \quad (12)$$

where  $K_S$  is the thermal conductivity of particles,  $T_j$  is jet temperature, and  $T_v$  is the temperature in the region near the jet. (Both temperatures are measured experimentally.) The heat transfer coefficient  $h$  is computed using the following expression (9):

$$\frac{hd_p}{k_g} = 2.0 + 0.6 \left( \frac{d_p \rho_g (v_g - v_p)}{\mu_g} \right)^{1/2} \left( \frac{c_p \mu_g}{k_g} \right)^{1/3} \quad (13)$$

where  $k_g$  is the gas thermal conductivity,  $v_g$  is the gas stream velocity,  $v_p$  is the particle velocity,  $d_p$  is the diameter of the particle,  $\mu_g$  is gas viscosity, and  $c_p$  is the specific heat.

Using the above heat and momentum equations, the temperature of a single particle  $T_p$  at any location near and in the jet can be calculated.

If the calculated temperature of the particles,  $T_p$ , in the jet zone reaches the melting temperature, the outer layer of the particles melt, and the particles may agglomerate upon collision. For each collision, there is only a finite probability of  $P^*$  leading to successful agglomeration.

The probability  $P^*$  is the fraction of all the collisions, which meet the following agglomeration criteria:

$$\begin{array}{l} \text{Relative Kinetic Energy} \\ \text{of Colliding Particles} \end{array} < \begin{array}{l} \text{Potential for Dissipation of the} \\ \text{Kinetic Energy due to Agglomeration} \end{array} \quad (14)$$

The relative kinetic energy of two colliding particles may be calculated from their velocities as -

$$\frac{1}{2} \frac{m_1 m_2}{m_1 + m_2} (v_1 - v_2)^2$$

where  $m_1$  and  $m_2$  are the masses of two particles with velocities  $v_1$  and  $v_2$ , respectively. (See the Appendix.) To calculate the potential of two particles for energy dissipation, the thickness of the molten layer (i.e., the layer with temperature higher than melting point) is denoted as  $\delta$  and may be calculated from the temperature distribution inside a particle at any location in the jet. We may write:

$$\text{Potential for Energy Dissipation} = 3\pi\mu_k |v_1 - v_2| \left( \frac{\delta_1 + \delta_2}{2} \right)^2 \quad (15)$$

where  $\mu_k$  is the viscosity of the molten layer and  $\delta_1$  and  $\delta_2$  are the thicknesses of molten layers on the surface of the two particles. (See the Appendix.) The criterion for agglomeration thus becomes:

$$\frac{1}{2} \frac{m_1 m_2}{m_1 + m_2} |v_1 - v_2| < 3\pi\mu_k \left( \frac{\delta_1 + \delta_2}{2} \right)^2 \quad (16)$$

Agglomeration Kinetics. In our agglomeration model, all particles are assumed to be spherical and have the same density. Agglomerates are formed by the collision of a pair of sticky particles. The volume number density  $n(I)$ , is defined as the number of size I particles per unit volume. The collision frequency between two particles of sizes I and J is proportional to their volume number densities and may be written as:

$$\left( \begin{array}{c} \text{Frequency of Collision} \\ \text{Between Particle Sizes I and J} \end{array} \right) = \beta_{I,J} n(I) n(J) \quad (17)$$

where  $\beta$  is the collision frequency constant. The agglomeration rate between size I particles and size J particles is expressed as:

$$R_{I,J} = P^* \beta_{I,J} n(I) n(J) \quad (18)$$

The volume number densities  $n(I)$  and  $n(J)$  may be expressed as:

$$n(I) = E_I N(I) \quad (19)$$

$$n(J) = E_J N(J) \quad (20)$$

where  $E_I$  and  $E_J$  are the coefficients of entrainment of particle sizes I and J into the jet. It is assumed that the size distribution of particles in the jet dilute phase remains the same as that in the fluidized bed. Therefore, the coefficients of entrainment for all particle sizes into the jet should be equal, as:

$$E_I = E_J = E \quad (21)$$

The agglomeration rate  $R_{I,J}$  may be written as:

$$R_{I,J} = P^* \beta_{I,J} E^2 N(I)N(J) \quad (22)$$

Comparing Equation 22 with Equation 2, the agglomeration rate constant may be written as:

$$K_{I,J} = P^* \beta_{I,J} E^2 \quad (23)$$

As previously mentioned,  $K_{I,J}$  can be represented by a multiple of two functions; one dependent on operating conditions and the other on size:

$$K_{I,J} = k_{op} (d_I^4 + d_J^4) \left( \frac{1}{d_I^3} + \frac{1}{d_J^3} \right) \quad (24)$$

The value of collision frequency constant  $\beta$  depends on the size of the colliding particles. If  $\beta$  dependency on particle size can be expressed with the same function as that for the agglomeration rate constant,

$$\beta_{I,J} = \beta' (d_I^4 + d_J^4) \left( \frac{1}{d_I^3} + \frac{1}{d_J^3} \right) \quad (25)$$

and we may then write:

$$k_{op} = P^* \beta' E^2 \quad (26)$$

The probability  $P^*$  in Equation 26 is the fraction of all the collisions that meet the agglomeration criteria in Equation 14. This probability is calculated by defining  $\xi$  as follows:

$$\xi = \begin{cases} 1 & \text{if two particles of size I and J meet the agglomeration criteria} \\ 0 & \text{if two particles of size I and J do not meet the agglomeration criteria} \end{cases}$$

The value of  $P^*$  is calculated as the number of collisions for which  $\xi = 1$  divided by the total number of collisions.

$\beta^2 E^2$  depends mainly on the gas and solid flow behavior in the fluidized bed. Our studies indicate that, for the runs with the same jet nozzle diameter and jet air velocity and approximately the same particle-size distribution,  $\beta^2 E^2$  has approximately the same value.

**Results and Discussion.** The values of  $k_{op}$  were calculated for different jet and fluidizing air temperatures at constant jet nozzle diameter, jet and fluidizing air velocities, and feed particle-size distribution using Equation 26 with the value of  $\beta^2 E^2$  set equal to  $1.35 \times 10^{-5}$ . This value of  $\beta^2 E^2$  was chosen so that the value of  $k_{op}$  evaluated from experimental data agreed with that calculated from the model, for the run conducted at the jet air temperature of  $144.4^\circ\text{C}$  and fluidizing air temperature of  $115.7^\circ\text{C}$ . The values of  $k_{op}$  calculated for other jet temperatures are shown in Table 2 which agree well with the values from the experimental data. The predicted values of  $k_{op}$  for different fluidizing air temperatures while maintaining constant jet temperature compare reasonably well with the experimental values (Table 3).

Table 2. THE PREDICTED VALUES OF  $k_{op}$  AT DIFFERENT JET TEMPERATURES AND A FLUIDIZING AIR TEMPERATURE OF  $115.7^\circ\text{C}$

Jet Temp, $^\circ\text{C}$	144.4	143.3	142.8	142.2
$k_{op}$ From Model	$1.78 \times 10^{-9}$	$1.20 \times 10^{-9}$	$0.89 \times 10^{-9}$	$0.63 \times 10^{-9}$
$k_{op}$ From Experiment	$1.78 \times 10^{-9}$	$1.20 \times 10^{-9}$	$0.90 \times 10^{-9}$	$0.45 \times 10^{-9}$

Table 3. THE PREDICTED VALUES OF  $k_{op}$  AT DIFFERENT FLUIDIZING AIR TEMPERATURES AND A JET TEMPERATURE OF  $144.4^\circ\text{C}$

Fluidizing Air Temp, $^\circ\text{C}$	115.7	104.6	93.5	82.3
$k_{op}$ From Model	$1.78 \times 10^{-9}$	$1.15 \times 10^{-9}$	$0.68 \times 10^{-9}$	$0.54 \times 10^{-9}$
$k_{op}$ From Experiment	$1.78 \times 10^{-9}$	$1.05 \times 10^{-9}$	$0.84 \times 10^{-9}$	$0.66 \times 10^{-9}$

#### REFERENCES

1. Arastoopour, H., Huang, C. S. and Weil, S. A., "Fluidization Behavior of Sticky Particles," Journal of Fine Particle Society (1986).
2. Arastoopour, H., Gu, A. Z. and Weil, S. A., "The Effect of Gas Distributors on the Agglomeration Process in Fluidized Beds," in the Proceedings of the 4th International Symposium on Agglomeration, 443-450, 1985.



3. Arastoopour, H., Weil, S. A., Huang, C. S. and Gu, A. Z., "A Fundamental Study in Support of the Understanding of the Agglomeration of Coal in Coal Gasifiers," in the Proceedings of the 20th Intersociety Energy Conversion Engineering Conference, Vol. 1, 1625-1630, 1985.
4. Gluckman, M. J., Yerushalmi, J. and Squire, A. M., "Defluidization Characteristics of Sticky or Agglomerating Beds," Fluidization Technology, Keairns, D., Ed., 2, 395 (1976).
5. Vora, M. K., Sandstrom, W. A. and Rehmat, A. G., "Ash Agglomeration in the Fluidized Bed." Paper presented at the Sixth National Conference on Energy and the Environment, Pittsburgh, May 21-24, 1979.
6. Hariri, H., Rehmat, A. and Arastoopour, H., "Temperature Distribution in a Fluidized Bed With a Central Jet." Paper presented at the A.I.Ch.E. Annual Meeting, New York, November 15-20, 1987.
7. Ricou, F. P. and Spalding, D. B., "Measurement of Entrainment by Axisymmetrical Turbulent Jets," Journal of Fluid Mechanics 11, 21-32 (1961).
8. Tatterson, D. C., Marker, T. L. and Forgacs, J. M., "Particle Effects on Free Jet Entrainment," The Canadian Journal of Chemical Engineering, 65:361-365 (1987).
9. Bird, R. B., Stewart, W. E. and Lightfoot, E. N., Transport Phenomena. New York: John Wiley & Sons, 1960.

#### APPENDIX

##### Relative Kinetic Energy of Colliding Particles

The compression action between the two collinear-colliding particles will keep on until the relative velocity between these two particles is zero. At this point, the deformation is at the maximum, as is the contact area between the two particles. However, the sum of the kinetic energies of the two particles reaches a minimum. This can be proved using the momentum balances for the collinear-colliding particles. The difference between the sum of the kinetic energies of the two particles before collision and that of the two particles at maximum deformation can be derived using the following assumptions. Assume that the velocities of two particles before collision with mass  $m_1$  and  $m_2$  are  $v_1$  and  $v_2$ , respectively. ( $v_1$  and  $v_2$  are collinear.) If the maximum deformation is achieved, these two particles will have the same velocity,  $v'$ . The momentum balance may be written as:

$$m_1 v_1 + m_2 v_2 = (m_1 + m_2) v'$$

The difference of the kinetic energies in these two states is:

$$\begin{aligned} & \frac{1}{2} m_1 v_1^2 + \frac{1}{2} m_2 v_2^2 - \frac{1}{2} (m_1 + m_2) v'^2 = \frac{1}{2} m_1 v_1^2 \\ & + \frac{1}{2} m_2 v_2^2 - \frac{1}{2} (m_1 + m_2) \left( \frac{m_1 v_1 + m_2 v_2}{m_1 + m_2} \right)^2 = \frac{1}{2} \frac{m_1 m_2}{m_1 + m_2} (v_1 - v_2)^2 > 0 \end{aligned}$$

##### Potential For Energy Dissipation in Particles

The potential dissipation capability is associated with the viscous dissipation of molten material on the surfaces of the colliding particles. The molten material is caused to flow relative to the surface mainly by the sudden particle velocity change and the compression action between particles during collision and, to a much

smaller degree, by the action of surface tension. As a first estimate, the flow of the molten layer is approximated by the viscous fluid (the creeping flow) over the spherical particles. Thus, the drag force exerted on the particles is calculated from the following equations (9).

$$F_n = \int_0^{2\pi} \int_0^\theta \left( \frac{3}{2} \frac{\mu_\ell v}{R} \cos^2 \theta' \right) R^2 \sin \theta' d\theta' d\phi = \pi \mu_\ell v R (1 - \cos^3 \theta)$$

$$F_t = \int_0^{2\pi} \int_0^\theta \left( \frac{3}{2} \frac{\mu_\ell v}{R} \sin^2 \theta' \right) R^2 \sin \theta' d\theta' d\phi = \pi \mu_\ell v R (2 - 3 \cos \theta + \cos^3 \theta)$$

where  $F_n$  and  $F_t$  are the summations of the projections of normal and tangential forces exerting on hard-core surface in the direction opposite to the particle flow direction.  $v$  is the characteristic velocity of the melted layer relative to the particle hard core.  $\mu_\ell$  is the viscosity of the melted material.

$$F_n + F_t = 3\pi \mu_\ell v R (1 - \cos \theta) = 3\pi \mu_\ell v R \frac{(\delta_1 + \delta_2)}{2R} = 3\pi \mu_\ell v \left( \frac{\delta_1 + \delta_2}{2} \right)$$

If the thicknesses of the melted layers are  $\delta_1$  and  $\delta_2$ , respectively, the energy dissipated due to viscous flow can be approximated as the product of force exerted on the particle hard core and the relative distance traveled between them.

$$\text{Potential Dissipation Capability} = (F_n + F_t) \times (\delta_1 + \delta_2) = 6\pi \mu_\ell v \left( \frac{\delta_1 + \delta_2}{2} \right)^2$$

It is further assumed that  $v$  is equal to the half of the relative velocity  $|v_1 - v_2|$  before particle collision; thus:

$$\text{Potential Dissipation Capability} = 3\pi \mu_\ell |v_1 - v_2| \left( \frac{\delta_1 + \delta_2}{2} \right)^2$$

#### ACKNOWLEDGMENT

This work was sponsored by the U.S. Department of Energy under Contract No. DE-AC21-87MC23283.

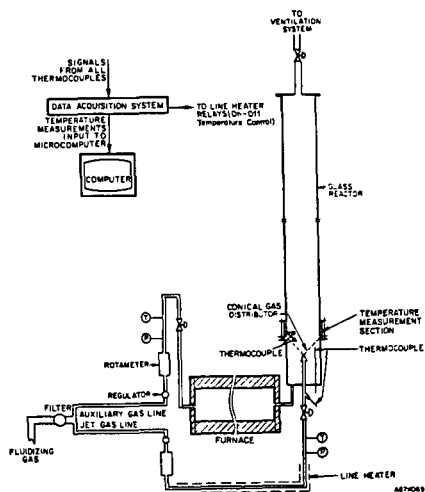


Figure 1. SCHEMATIC DIAGRAM OF THE EXPERIMENTAL SETUP

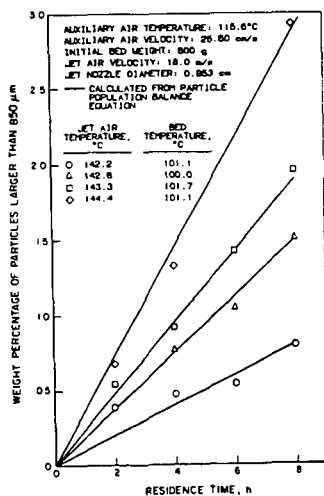


Figure 2. COMPARISON OF WEIGHT PERCENTAGES OF PARTICLES LARGER THAN 850  $\mu\text{m}$  CALCULATED FROM THE PARTICLES' POPULATION BALANCE EQUATION AND EXPERIMENTAL DATA AT FOUR DIFFERENT JET AIR TEMPERATURES

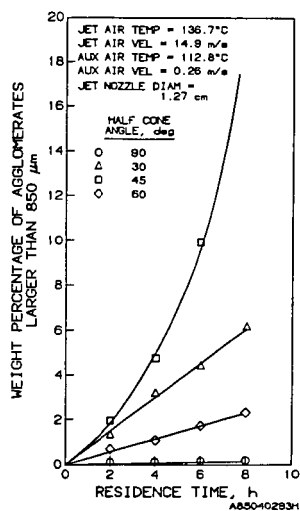


Figure 3. COMPARISON OF WEIGHT PERCENTAGES OF AGGLOMERATES WITH FOUR DIFFERENT CONE ANGLE GAS DISTRIBUTORS

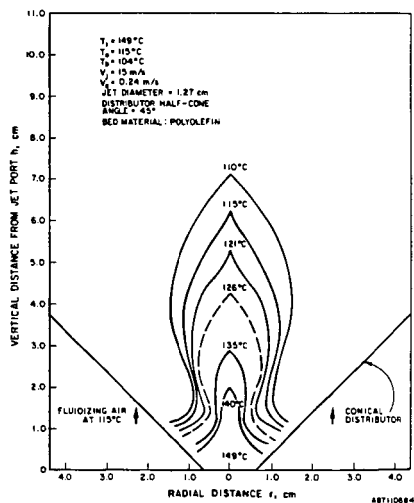


Figure 4. JET ZONE ISOTHERMS IN A FLUIDIZED BED AT A JET AIR TEMPERATURE OF 149°C AND A FLUIDIZING AIR TEMPERATURE OF 115°C